



## JRC TECHNICAL REPORTS

# Development and test of the high-precision $\gamma$ -beam monitor at the ESFRI facility ELI-NP

Göök A., Oberstedt S., Geerts W.,  
Hamsch F.-J.

Public

2017

This publication is a Technical report by the Joint Research Centre (JRC), the European Commission's science and knowledge service. It aims to provide evidence-based scientific support to the European policymaking process. The scientific output expressed does not imply a policy position of the European Commission. Neither the European Commission nor any person acting on behalf of the Commission is responsible for the use that might be made of this publication.

#### **Contact information**

Name: S. Oberstedt  
Address: JRC-Geel, Retieseweg 111, B-2440 Geel, Belgium  
Email: Stephan.Oberstedt@ec.europa.eu  
Tel.: +32 14 571361

#### **JRC Science Hub**

<https://ec.europa.eu/jrc>

JRC109694

EUR 29002 EN

PDF ISBN 978-92-79-77287-0 ISSN 1831-9424 doi:10.2760/367216

Luxembourg: Publications Office of the European Union, 2017

© European Atomic Energy Community, 2017

Reuse is authorised provided the source is acknowledged. The reuse policy of European Commission documents is regulated by Decision 2011/833/EU (OJ L 330, 14.12.2011, p. 39).

For any use or reproduction of photos or other material that is not under the EU copyright, permission must be sought directly from the copyright holders.

How to cite this report: Göök A., Oberstedt S., Geerts W., Hamsch F.-J., *Development and test of the high-precision  $\gamma$ -beam monitor at the ESFRI facility ELI-NP*, EUR (where available), Publications Office of the European Union, Luxembourg, 2017, 978-92-79-77287-0, doi 10.2760/367216, PUBSY No. 109694

All images © European Atomic Energy Community 2017

**Title** Development and test of the high-precision gamma-beam monitor at the ESFRI facility ELI-NP

**Abstract**

*This document describes the development of a fission chamber for gamma beam intensity monitoring at the high-energy gamma line at ELI-NP*

*The fission chamber foreseen for monitoring the gamma beam intensity on the high-energy beam line at ELI-NP is an ionization chamber with several  $^{238}\text{U}$  deposits of a thickness in the range from 100 to 150  $\mu\text{g}/\text{cm}^2$  in a compact design.*

# Contents

- Acknowledgements ..... 1
- Abstract ..... 2
- 1 Introduction ..... 3
- 2 Fission chamber design ..... 5
- 3 Cf-252 test chamber ..... 7
  - 3.1 Experimental Results..... 7
    - 3.1.1 Timing Properties..... 7
    - 3.1.2 Fission Counting Properties ..... 9
- 4 Discussion ..... 12
- 5 Conclusions ..... 13
- References ..... 14
- List of figures ..... 15
- List of tables ..... 16

## **Acknowledgements**

The authors acknowledge the support of the sample preparation group for the delivery of the high quality  $^{238}\text{U}$  targets

### ***Authors***

Göök A.

Geerts W.

Hamsch F.-J.

Oberstedt S.

## **Abstract**

This document describes the development of a fission chamber for gamma beam intensity monitoring at the high-energy gamma line at ELI-NP

The fission chamber foreseen for monitoring the gamma beam intensity on the high-energy beam line at ELI-NP is an ionization chamber with several  $^{238}\text{U}$  deposits of a thickness in the range from 100 to 150  $\mu\text{g}/\text{cm}^2$  in a compact design. The innovative design of the chamber allows measuring for each individual micro pulse arriving at a time interval of  $1.6 \times 10^{-8}$  s.

# 1 Introduction

The high brilliance Gamma Beam System (GBS) at ELI-NP will deliver quasi-monochromatic gamma-ray beams with a high spectral density and high degree of linear polarization [1]. The GBS will be delivered in two phases with two separate beam lines: a low-energy gamma-ray line with gamma energies up to 3.5 MeV and a high-energy gamma line with energies up to 19.5 MeV. Optimization and monitoring of the gamma beam with these characteristics is challenging and requires the proper means for accurately measuring the spatial, spectral and temporal characteristics of the gamma-ray beams.

The parameters of the GBS are listed in Table 1. These parameters of the gamma beam have to be achieved for the full system, which will be operational in the second half of 2018.

**Table 1:** Parameters of the ELI-NP gamma-ray beam.

Parameter [units]	Value
Photon energy [MeV]	0.2 – 19.5
Spectral density [ph/s/eV]	$> 10^4$
Bandwidth	$< 0.5 \%$
# photons per shot within FWHM bdw.	$1.0 - 4.0 \times 10^5$
# photons/sec within FWHM bdw.	$2.0 - 8.0 \times 10^8$
Source rms size [ $\mu\text{m}$ ]	10 – 30
Source rms divergence [ $\mu\text{rad}$ ]	25 – 250
Peak brilliance [ $N_{\text{ph}}/\text{sec} \cdot \text{mm}^2 \cdot \text{mrad}^2 \cdot 0.1\%$ ]	$10^{22} - 10^{24}$
Radiation pulse length [ps]	0.7 – 1.5
Linear polarization	$> 99 \%$
Macro repetition rate [Hz]	100
# of pulses per macropulse	$> 31$
Pulse-to-pulse separation [ns]	16

This document describes the development of a fission chamber for gamma beam intensity monitoring at the high-energy gamma line at ELI-NP.

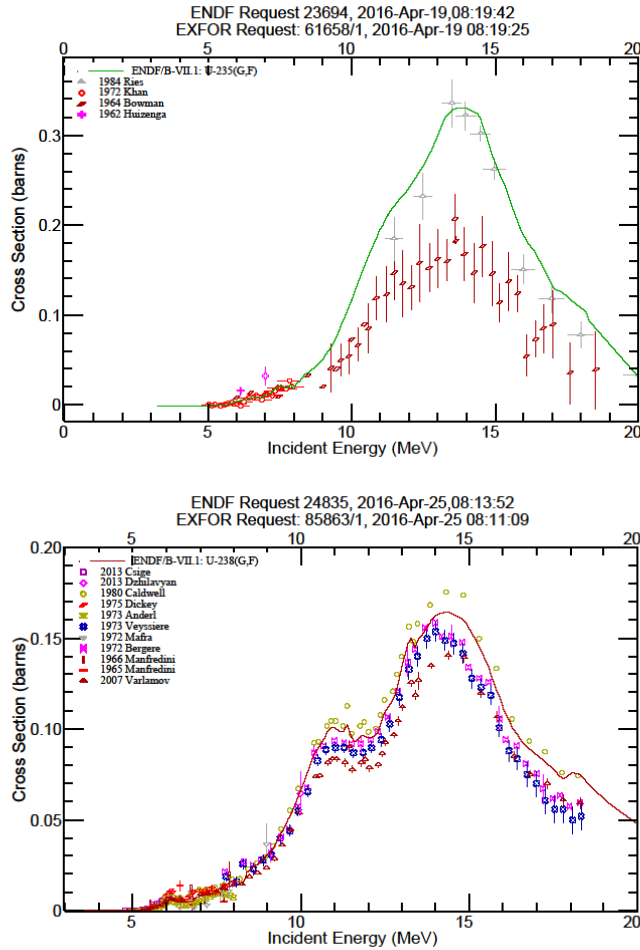


**Figure 1:** Photofission cross sections for  $^{235}\text{U}$  (top) and  $^{238}\text{U}$  (bottom). Experimental data from the EXFOR library (The data marked 2007 Varlamov is an evaluation) compared to ENDF/B-VII.1

The fission chamber foreseen for monitoring the gamma beam intensity on the high-energy beam line at ELI-NP will be an ionization chamber with a  $^{238}\text{U}$  deposit of a thickness in the range from 100 to 150  $\mu\text{g}/\text{cm}^2$ . The thickness should allow an average counting rate of about 100 Hz. In Figure 1 the photo-fission cross section of  $^{235}\text{U}$  and  $^{238}\text{U}$  is displayed. The ENDF/B-VII.1 evaluation shows a larger cross section for  $^{235}\text{U}(\gamma, f)$ . However, the experimental data on the  $^{238}\text{U}(\gamma, f)$  cross section is in better accordance and with smaller uncertainties. This is why we have chosen to base the monitor on a  $^{238}\text{U}$  deposit.

## 2 Fission chamber design

The gamma beam consists of 100 macro-pulses per second, each macro-pulse formed of 32 pulses separated by 16 ns. This temporal structure needs to be accounted for when estimating the count rates in the fission chamber. In particular, the probability of pile-ups in the ionization chamber needs to be considered if the detector is not fast enough to resolve the temporal structure of the beam. Consider a parallel plate ionization chamber with a 7 mm inter-electrode gap filled with P-10 gas. The electron drift velocity is about 0.05 mm/ns, giving a charge collection time of 140 ns. This defines the detectors resolving time. For an event occurring at  $t = 0$ , the probability of having a pile-up can be calculated according to

$$P_{\mu}(x > 0) = 1 - P_{\mu}(0),$$

where  $P_{\mu}(x)$  is the Poisson distribution with  $\mu$  expected average counts. Here  $\mu$  is taken as the expected number of fissions per micro pulse times the number of micro pulses contained within the resolving time of the fission chamber. Figure 2 shows the pile up probability as a function of the gamma ray energy calculated for a  $400 \mu\text{g}/\text{cm}^2$  thick  $^{238}\text{U}$  target. It should be mentioned that this calculation does not take into account the macro pulse structure, the probability of pile up will diminish towards the end of a macro pulse.

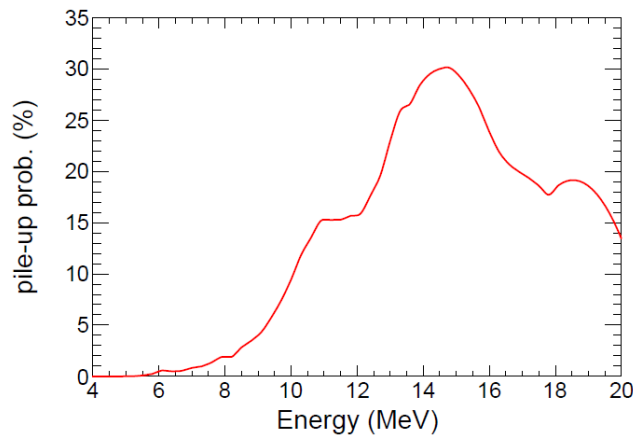


**Figure 2:** Probability of fission pile-up in a conventional ionization chamber with a  $400 \mu\text{g}/\text{cm}^2$  thick  $^{238}\text{U}$  target.

For a measured rate  $m$  a dead time correction could be applied to account for the pile up loss, obtaining a true rate

$$n = \frac{m}{P_{\mu}(0)}.$$

This equation is valid for a paralyzable system [2]. The correction factor  $P_{\mu}(0)$  must be calculated iteratively from the measured rate. The statistical uncertainty in the obtained true count rate scales as the square of the correction factor. Hence, for a pileup probability of about 30% the required measurement time will be twice as long as it would be if the signals were pile up free. The procedure of calculating the correction factor iteratively will add additional uncertainty, if the rate is highly variable during the measurement. Hence the pile-up rate should be kept as low as possible.



The pile-up rate can be diminished by adjusting the design parameters of the ionization chamber. First of all, a counting gas with a faster drift velocity should be considered. The gas  $\text{CF}_4$  is a commonly used counting gas, with a drift velocity of about 0.1 mm/ns. This gas also has a higher stopping power than P-10. Therefore, the inter electrode gap can be made smaller. Based on SRIM [3], the energy loss of typical fission fragments in a 1 mm thick layer of  $\text{CF}_4$  at atmospheric pressure is about 17 MeV. This is enough to separate fission events from the 4.4 MeV alpha particle background from the decay of  $^{238}\text{U}$ . With these design parameters the charge collection time reduces to 10 ns and the temporal structure of the beam could be resolved.

### 3 Cf-252 test chamber

Based on the above considerations a  $^{252}\text{Cf}$  chamber was assembled for initial tests. A schematic view and a photo of the test setup are displayed in Figure . The  $^{252}\text{Cf}$  sample is located in a 10 mm diameter active spot on a 25 mm diameter stainless steel disc with a thickness of 0.18 mm. In order to preserve the fast timing properties of the detector a wide band current sensitive preamplifier (CAEN A1423) was connected to the sample disc. A negative bias is applied via the preamplifier to the sample disc in order to repel the ionisation electrons. The electrons are then collected on the opposite grounded electrode. The electron collector is separated from the sample by 1 mm. The test chamber was operated with constant flow of ca. 30 ml/min  $\text{CF}_4$ . The flow rate was controlled with a needle valve, while the pressure was controlled using a digital pressure controller. The gas flow was monitored at both the input and output stages, in order to ensure that no air contamination enters into the ionisation chamber volume. In order to be able to test the chamber at pressures below ambient pressure a vacuum pump was attached at the end of the gas flow line. For the purpose of the tests the output of the preamplifier was digitized at a rate of 1.8 GS/s.

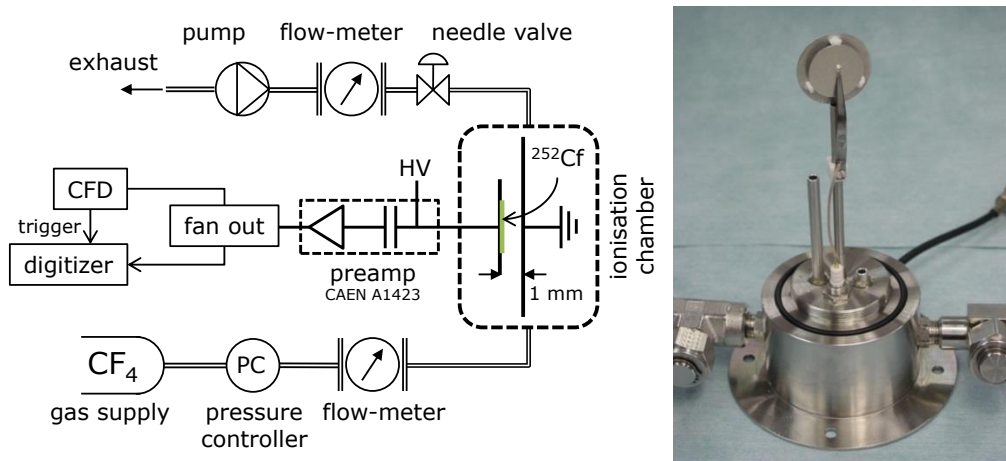


**Figure 3:** Left: Schematic view of the experimental setup used for the tests. Right: Photo of the Cf-252 ionisation chamber with the cover removed

## 3.1 Experimental Results

### 3.1.1 Timing Properties

In order to determine the correct biasing voltage data was first obtained at varying bias with the chamber operated at a gas pressure of 1.0 bar. In the upper part of Figure 4 the average signal width (at 5 % of the signal amplitude) is plotted as a function of the reduced field strength. The signal width decreases with increasing biasing voltage, as expected from the relationship between reduced field strength and drift velocity. A reduced field-strength of 2 kV/cm/bar is enough to obtain signals with a width below 10 ns. A typical digitized fission signal from the ionization chamber is also displayed in the lower part of Figure 4. This signal was obtained at 1 bar of gas pressure and a bias of -300 V. The signal is well separated from the electronic noise and has a width below 10 ns.

The timing resolution of the detector was tested by measuring prompt fission gamma rays with a liquid scintillator in coincidence with the fission trigger. The width of the prompt fission gamma ray peak in the time of flight spectrum is 0.9 ns FWHM. Correcting for the timing resolution of the liquid scintillator a resolution of ca. 0.7 ns FWHM for the ionisation chamber is obtained. These properties ensure that the time structure of the

gamma-ray beam at ELI-NP can be resolved without problems. Figure 5 shows the pile up probability as a function of the gamma ray energy calculated for a  $400 \mu\text{g}/\text{cm}^2$  thick  $^{238}\text{U}$  target based on a pulse width of 10 ns.

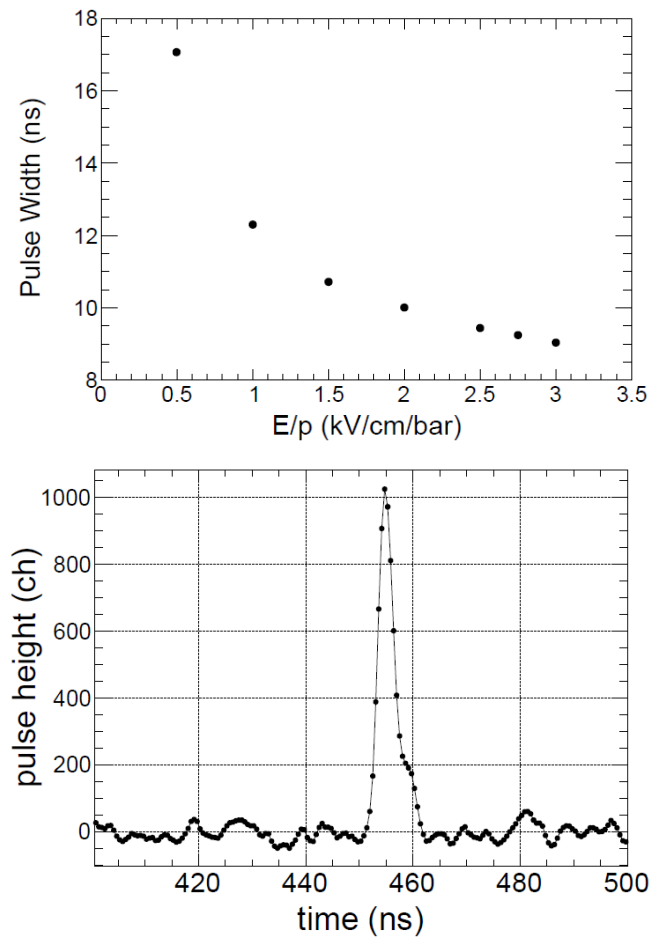


**Figure 4:** Top: Signal width as a function of the reduced field strength. Bottom: typical fission signal from the ionisation chamber.

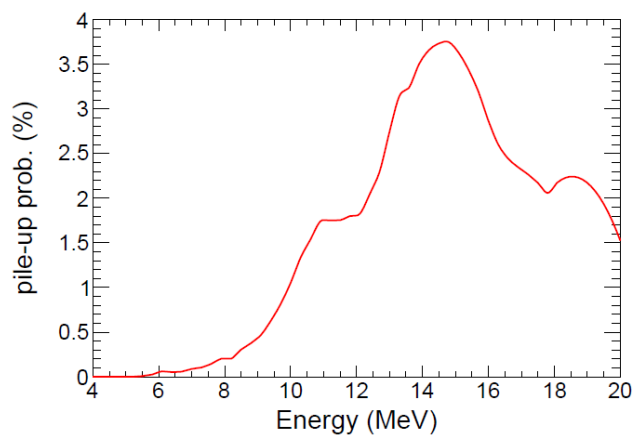


**Figure 5:** Probability of fission pile-up in an ionization chamber with a pulse width of 10 ns and with a  $400 \mu\text{g}/\text{cm}^2$  thick  $^{238}\text{U}$  target.

### 3.1.2 Fission Counting Properties

On the left hand side of Figure 6 pulse height distributions obtained from the ionisation chamber at a pressure of 1 bar at varying biasing voltages are displayed on the left hand side. Two distinctly different types of events can be identified; alpha-particle induced events at low pulse heights and fission induced events at higher pulse heights. It is necessary to apply a pulse height threshold in order to discriminate between alpha particle induced and fission induced signals. On the right hand side of Figure 6 the average pulse height is displayed as a function of the reduced field strength. It is observed that for increasing biasing voltage the distributions shift towards higher pulse heights, but also that the overlap of the alpha particle distribution and the fission distribution becomes smaller. Above a biasing voltage of -275 V, corresponding to a reduced field strength of 2.75 kV/cm/bar, the change is minimal. The final biasing voltage has been chosen at -300 V, corresponding to 3.0 kV/cm/bar.

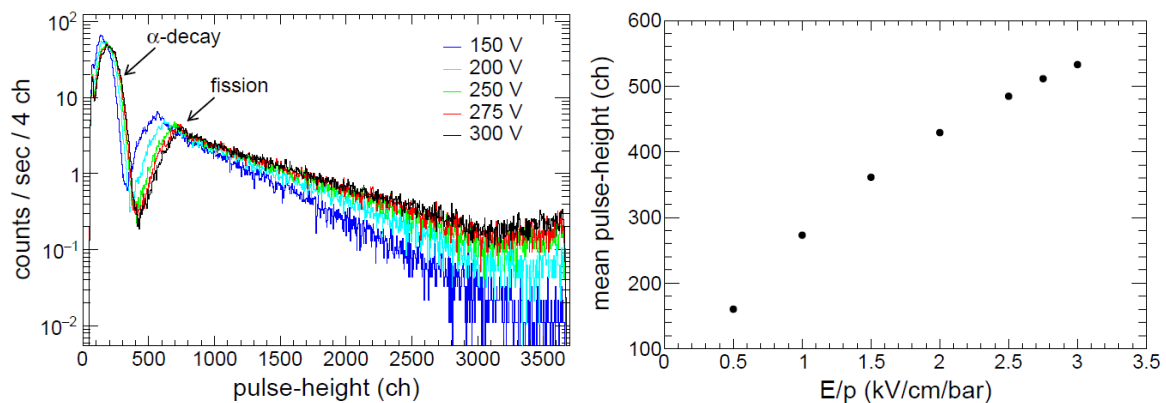


**Figure 6:** Left: Pulse-height distributions for different biasing voltages. Right: Mean pulse-height as a function of the reduced field strength.

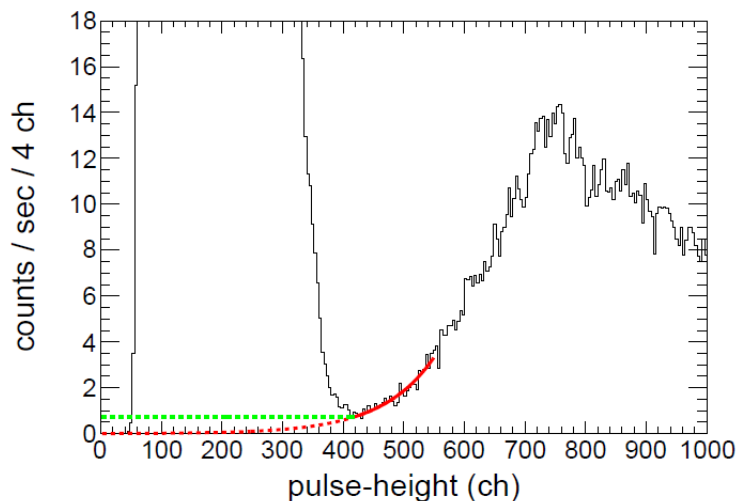


**Figure 7:** Two extrapolation schemes for determining the total fission activity of the <sup>252</sup>Cf sample. The dashed red line shows the extrapolation of the fitted exponential, indicated by the full red line, from pulse height threshold down to zero. The green dashed line assumes a constant rate per channel equal to the value of the fitted exponential at the pulse height threshold. The data is taken at a gas pressure of 1 bar, with a reduced field strength of 3 kV/cm/bar.

The missing part of the fission distribution below the threshold must be taken into account when determining the fission activity of the sample. The shape of the fission fragment pulse height distributions at low energy deposits in parallel plate ionisation chambers has been studied in detail in Ref.[4].

It has been shown that, for a biasing configuration where the electrons are collected on the opposite electrode to where the sample is located, no increase in fission count-rate is to be expected towards zero pulse height. For the present study we have used two extreme cases for extrapolating the fission distribution to zero pulse height, as illustrated in Figure 7.

- 1.) An exponential fit is applied to the rising edge of the fission distribution. The integral of the fitted exponential from zero to threshold gives a lower limit for the number of fissions below the pulse height threshold.
- 2.) An upper limit for the number of fissions below the pulse height threshold is derived by assuming a constant fission rate per channel below the threshold. The constant rate is taken from the value of the exponential fit at the threshold.

The final value for the number of fissions lost below the threshold is taken as the mean between the two extreme cases, and the uncertainty in this value is taken as half of the difference between them. The magnitude of this systematic uncertainty is about 1 % of the determined total activity.

It is expected that a change in the gas pressure will affect the shape of the pulse-height distribution, since the energy lost in the gas by the ionising particle will be different. To investigate possible systematic effects of this on the determination of the fission activity the chamber was tested with a number of different gas pressures ranging from 0.5 bar to 1.2 bar. For each gas pressure the biasing voltage was adjusted in order to maintain the same reduced field strength of 3 kV/cm/bar. In Figure 8 pulse height distributions for four different gas pressures are displayed. As expected, the lower the pressure is the lower is the pulse height. However, in the range 0.7 bar to 1.2 bar the count rate where the alpha particle and the fission distributions meet is remarkably constant. For each of the measurements the procedure for extrapolating the fission distribution to zero pulse height was repeated. The results are summarized in Table 2 and represented graphically in Figure 9. The deviations of the results are below 1%, and compatible with the statistical uncertainty of the fission counting. The average value ( $2800 \pm 30$ ) fissions/s agrees within the uncertainty with the reference value ( $2776 \pm 20$ ) fissions/s, calculated from the measured fission activity of the sample [5]. The slight overestimate might be related to alpha particle induced events resulting in pulse heights above the threshold.

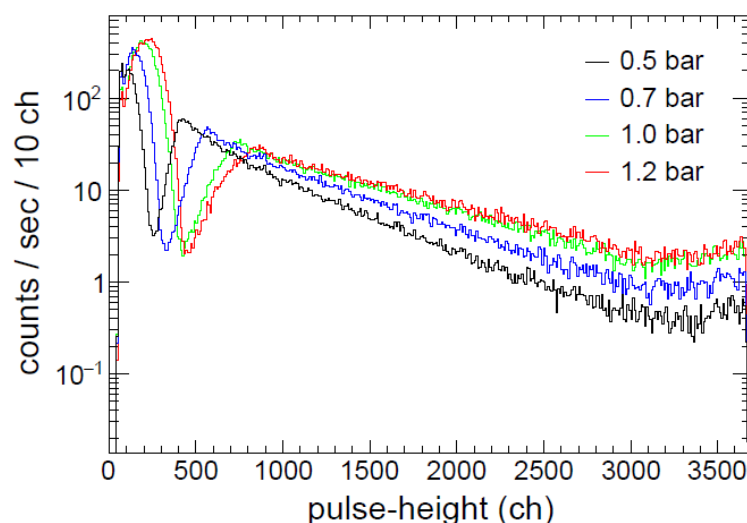


**Figure 8:** Pulse-height distributions for different gas pressures.

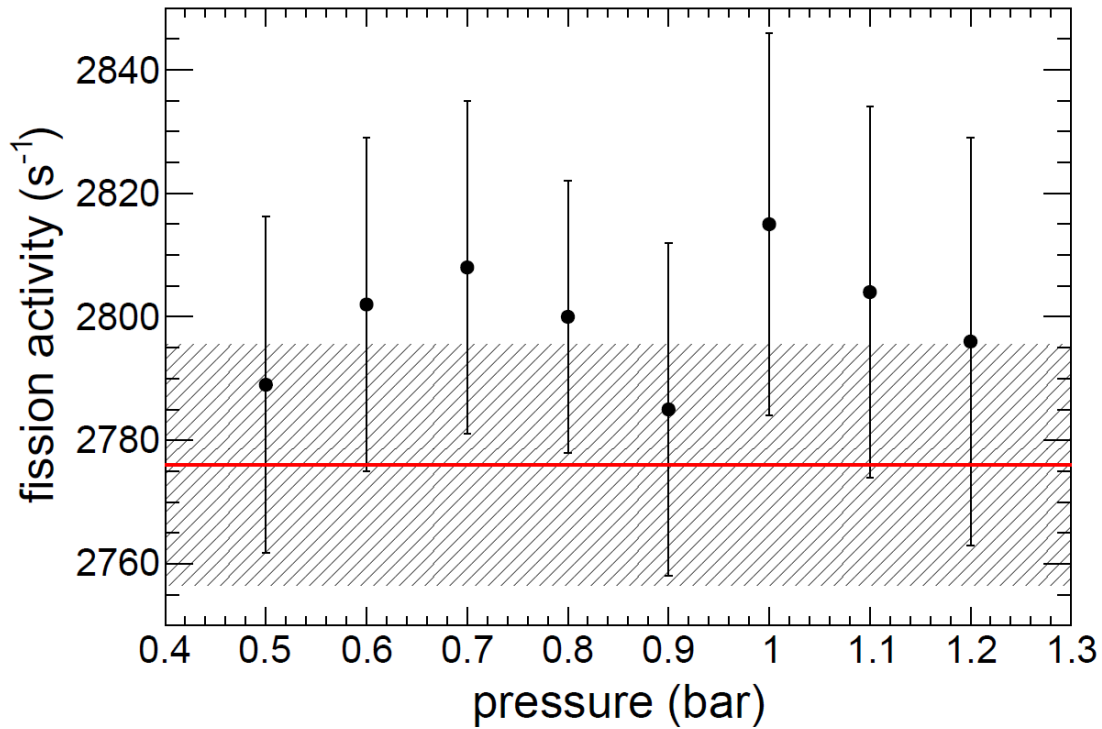


**Figure 9:** The determined fission activity of the sample as a function of the gas pressure in the ionization chamber; the solid red line and hatched area indicates the reference activity [5] and its uncertainty, respectively.

**Table 2:** Results on the fission activity determined at different gas pressure in the ionization chamber.

Pressure (mbar)	Bias (V)	Fission Rate (s <sup>-1</sup> )
500	-150	(2789±28)
600	-180	(2802±27)
700	-210	(2808±27)
800	-240	(2800±22)
900	-270	(2785±27)
1000	-300	(2815±31)
1100	-330	(2804±30)
1200	-360	(2796±33)

## 4 Discussion

The tests of the fast ionization chamber design based on an inter electrode gap of 1 mm and  $\text{CF}_4$  as counting gas has shown excellent properties in terms of timing. The short charge collection time, smaller than 10 ns, ensures that the temporal micro-pulse structure of the gamma-ray beam at ELI-NP can be resolved. This fact reduces the pile-up probability per detected fission event by 1 order of magnitude compared to a more conventional chamber design. The draw back with this design is that the overlap between alpha particle induced and fission induced pulses become larger. This does however not increase the uncertainty in the fission counting efficiency to more than 1 % for the  $^{252}\text{Cf}$  source. It is expected that the overlap between fission and alpha events will be smaller in the  $^{238}\text{U}$  ionization chamber. This is because the alpha activity of the foreseen samples are  $\sim 10^4$  times smaller than for the  $^{252}\text{Cf}$  sample and that the alpha particle energies from the foreseen samples are ca 30% lower, while the fission fragment energy in  $^{238}\text{U}(\gamma, f)$  are only ca. 8% lower than in  $^{252}\text{Cf}(sf)$ . On the other hand, the thickness of the  $^{238}\text{U}$  deposit will be greater than that of the  $^{252}\text{Cf}$  source; this will lead to a larger loss of fission events below the threshold. In addition, scattering inside the sample may lead to losses of fission fragments that do not escape the target layer. The contribution of these effects to the systematic uncertainty in the fission counting will have to be investigated with the final chamber and the actual  $^{238}\text{U}$  deposits.

## 5 Conclusions

Based on the tests a design of the ELI-NP chamber has been prepared and a prototype produced. An image of the chamber interior is shown in Fig. 10. This chamber will be used for tests at ELI-NP as soon as the facility is operational.

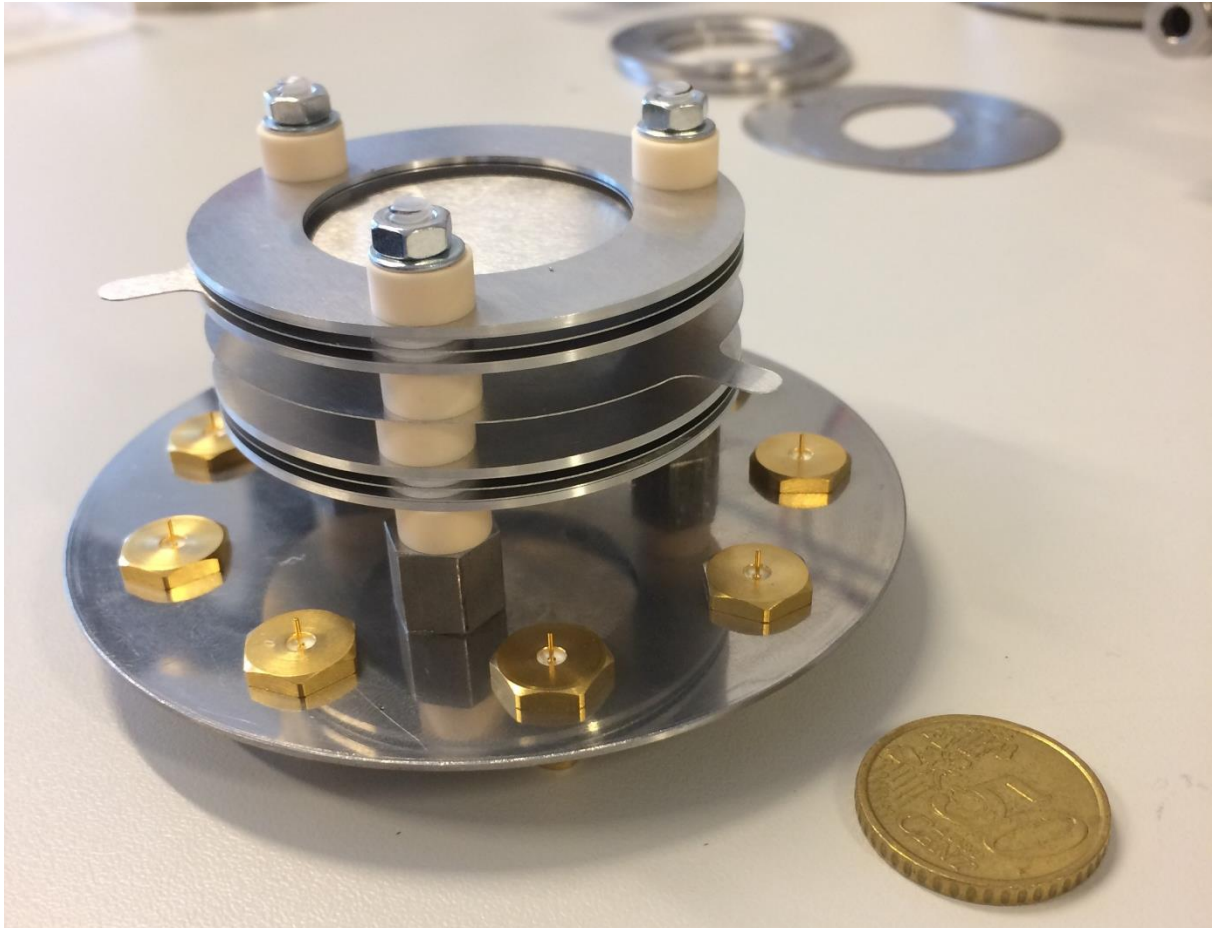


Figure 10: View onto the interior of the prototype ELI-NP high-precision photon-beam monitor.



## References

- [1] The White Book of ELI Nuclear Physics, Bucharest–Magurele (2010).
- [2] G.F. Knoll, Radiation Detection and Measurement, 3<sup>rd</sup> ed. (1999) ISBN 978-0-471-07338-3.
- [3] J.F. Ziegler, SRIM-2013, <http://www.srim.org/>.
- [4] A. Plompen, A. Negret, JRC Sci. Tech. Report, EUR 25208 EN (2011).
- [5] N.V.Kornilov, et al. Nucl. Instr. Meth. A 599 (2009) 226–233.

## List of figures

<b>Figure 1.</b> Photofission cross sections for $^{235}\text{U}$ (top) and $^{238}\text{U}$ (bottom). Experimental data from the EXFOR library (The data marked 2007 Varlamov is an evaluation) compared to ENDF/B-VII.1 .....	<b>4</b>
<b>Figure 2.</b> Probability of fission pile-up in a conventional ionization chamber with a $400\ \mu\text{g}/\text{cm}^2$ thick $^{238}\text{U}$ target .....	<b>5</b>
<b>Figure 3.</b> Left: Schematic view of the experimental setup used for the tests. Right: Photo of the Cf-252 ionisation chamber with the cover removed .....	<b>7</b>
<b>Figure 4.</b> Top: Signal width as a function of the reduced field strength. Bottom: typical fission signal from the ionisation chamber .....	<b>8</b>
<b>Figure 5.</b> Probability of fission pile-up in an ionization chamber with a pulse width of 10 ns and with a $400\ \mu\text{g}/\text{cm}^2$ thick $^{238}\text{U}$ target .....	<b>8</b>
<b>Figure 6.</b> Left: Pulse-height distributions for different biasing voltages. Right: Mean pulse-height as a function of the reduced field strength .....	<b>9</b>
<b>Figure 7.</b> Two extrapolation schemes for determining the total fission activity of the $^{252}\text{Cf}$ sample. The dashed red line shows the extrapolation of the fitted exponential, indicated by the full red line, from pulse height threshold down to zero. The green dashed line assumes a constant rate per channel, equal to the value of the fitted exponential at the pulse height threshold. The data is taken at a gas pressure of 1 bar, with a reduced field strength of 3 kV/cm/bar .....	<b>9</b>
<b>Figure 8.</b> Pulse-height distributions for different gas pressures .....	<b>10</b>
<b>Figure 9.</b> The determined fission activity of the sample as a function of the gas pressure in the ionization chamber; the solid red line and hatched area indicates the reference activity [5] and its uncertainty, respectively .....	<b>11</b>
<b>Figure 10.</b> View onto the interior of the prototype ELI-NP high-precision photon-beam monitor .....	<b>13</b>

## List of tables

<b>Table 1.</b> Parameters of the ELI-NP gamma-ray beam .....	<b>3</b>
<b>Table 2.</b> Results on the fission activity determined at different gas pressure in the ionization chamber .....	<b>11</b>

## **GETTING IN TOUCH WITH THE EU**

### **In person**

All over the European Union there are hundreds of Europe Direct information centres. You can find the address of the centre nearest you at: <http://europa.eu/contact>

### **On the phone or by email**

Europe Direct is a service that answers your questions about the European Union. You can contact this service:

- by freephone: 00 800 6 7 8 9 10 11 (certain operators may charge for these calls),
- at the following standard number: +32 22999696, or
- by electronic mail via: <http://europa.eu/contact>

## **FINDING INFORMATION ABOUT THE EU**

### **Online**

Information about the European Union in all the official languages of the EU is available on the Europa website at: <http://europa.eu>

### **EU publications**

You can download or order free and priced EU publications from EU Bookshop at: <http://bookshop.europa.eu>. Multiple copies of free publications may be obtained by contacting Europe Direct or your local information centre (see <http://europa.eu/contact>).

## JRC Mission

As the science and knowledge service of the European Commission, the Joint Research Centre's mission is to support EU policies with independent evidence throughout the whole policy cycle.



**EU Science Hub**  
[ec.europa.eu/jrc](https://ec.europa.eu/jrc)



@EU\_ScienceHub



EU Science Hub - Joint Research Centre



Joint Research Centre



EU Science Hub



Publications Office

doi:10.2760/367216

ISBN 978-92-79-77287-0